SUPPLEMENTAL MATERIAL

A. Molecular orientation in an electric field

The field-free Hamiltonian for the electronic ($^2\Sigma$) and vibrational ($v = 0$) ground state of a molecule such as ^{174}Yb^{107}Ag is

$$H_0 = B_{\rm rot} N(N+1) + \gamma \vec{S}\cdot\vec{N} + b\vec{S}\cdot\vec{I} + cS_zI_z, \tag{5}$$

where $\vec{N}, \vec{S}, \vec{I}$ are the molecular rotational angular momentum, electron spin and nuclear spin respectively. $B_{\rm rot}$ is the rotational constant of the molecule, γ is the spin-rotation parameter, and b, c are hyperfine interaction parameters. The interaction Hamiltonian with an electric field [see Eq. (1)] is $H_{\rm int} = -D\hat{n}\cdot\vec{\mathcal{E}}$, where D is the molecular dipole moment. The characteristic scale of the electric field needed to polarize the molecule is $\mathcal{E}_{\rm pol} = 2B_{\rm rot}/D$.

The spectroscopic constants for the YbAg molecule have yet to be measured, so for our calculations we estimated the values of $B_{\rm rot}, \gamma, b, c$ and D using the measured values for the structurally very similar molecule ^{174}Yb^{19}F [38]. We assume that the bond length and molecular dipole moment in YbAg are similar to that of YbF. The value of $B_{\rm rot}$ was scaled from that of YbF by the ratio of the reduced masses of Yb-Ag and Yb-F. The values of b and c were scaled from the YbF values by the ratio of the nuclear magnetic moments of ^{107}Ag and ^{19}F. We find that $\mathcal{E}_{\rm pol} \approx 2$ kV/cm for YbAg.

We used an uncoupled computational basis $|N, m_N; S, m_S; I, m_I\rangle$, including rotational levels up to $N = 20$, and numerically diagonalized $H_0 + H_{\rm int}$ for different values of $\mathcal{E}_z$. The resulting dependence of the molecular orientation $\zeta = \langle\hat{n}\cdot\hat{z}\rangle$ is shown in Fig. 4. The main features of the ζ vs. $\mathcal{E}_z$ curve can be understood from the simple approximate expression derived in Section B. When the calculated curve of ζ versus $\mathcal{E}_z$ is applied to a sinusoidal electric field $\mathcal{E}_z(t) = \mathcal{E}_0\cos(\omega t + \beta)$ (with $\mathcal{E}_0 = 3\mathcal{E}_{\rm pol}$), the curve for $\zeta(t)$ shown in Fig. 1 is obtained.

We also used the numerical model to calculate systematic errors, such as the $E1-M1$ mixing-induced Rabi frequency Ω_{E1-M1} described in the main text. For example, the numerical calculations confirm the estimate from perturbation theory, $\Omega_{E1-M1} \sim D\mathcal{E}_0\, D\mathcal{E}_{\rm dc}\, g_S\mu_B\mathcal{B}_{\rm dc}\, \frac{\gamma^2}{B_{\rm rot}^4}$.

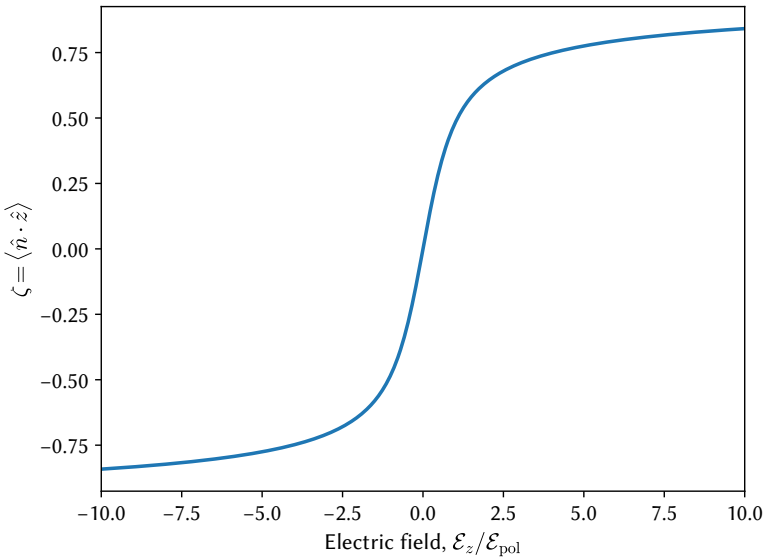

FIG. 4: Molecular orientation $\zeta = \langle\hat{n}\cdot\hat{z}\rangle$ as a function of the electric field applied to the molecule.

B. Analytical expression for ζ in a two-level system

The quantity ζ quantifies the orientation of a polar molecule along an applied electric field. In the main text, we numerically calculate ζ from the Hamiltonian in Equation (1) by considering the first 20 rotational levels. However,

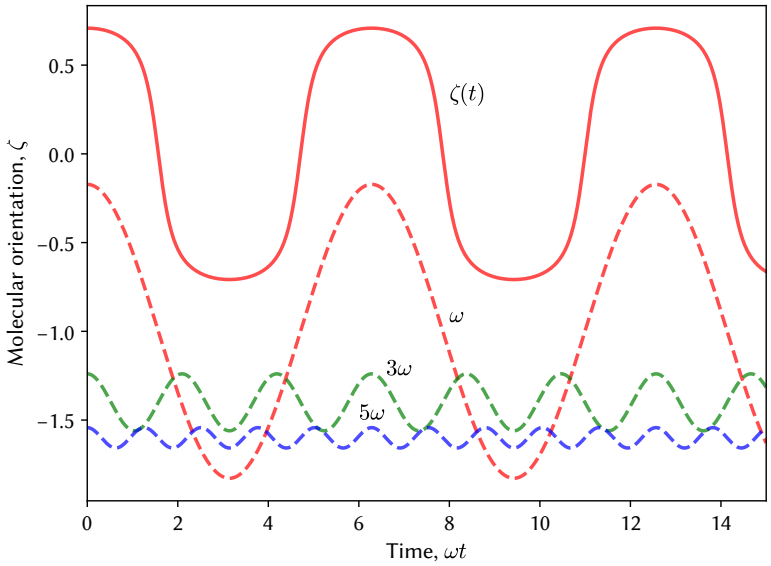

FIG. 5: Molecular orientation $\zeta = \langle \hat{n} \cdot \hat{z} \rangle$ in response to an electric field $\mathcal{E}_z(t) = 3\mathcal{E}_{\rm pol} \cos \omega t$. The harmonics contained in $\zeta(t)$ are offset for clarity.

some useful intuition for this quantity can be gained from an approximate analytical expression for the lowest pair of (opposite parity) rotational states, $|0\rangle \equiv |N = 0\rangle$ and $|1\rangle \equiv |N = 1, m_N = 0\rangle$. The Hamiltonian matrix for this two-level rotor system in an electric field is

$$H = \begin{pmatrix} -\omega_{01}/2 & -D_{01}\mathcal{E}_z \\ -D_{01}\mathcal{E}_z & \omega_{01}/2 \end{pmatrix} \tag{6}$$

where $D_{01} = \langle 0|D_z|1\rangle$ and ω_{01} is the spacing between $|0\rangle$ and $|1\rangle$. Typical rotational level spacing in polar molecules ($\omega_{01} \sim 2\pi\times$ 10 GHz) are much larger than the electric field drive frequency ($\omega \sim 2\pi\times$ 100 MHz, near the hyperfine resonance frequency). Therefore, a rotating wave approximation is not valid in this regime, and a better description of the dynamics results from a quasi-static (i.e., adiabatic) approximation. Therefore, we solve for ζ using the eigenvectors of the above Hamiltonian, assuming that $\mathcal{E}_z(t)$ varies slowly compared to the phase of the wavefunction ($\omega \ll \omega_{01}$).

The eigenvectors of the Hamiltonian are then $\left|\widetilde{0}\right\rangle = \cos(\frac{\theta}{2})|0\rangle - \sin(\frac{\theta}{2})|1\rangle$ and $\left|\widetilde{1}\right\rangle = \cos(\frac{\theta}{2})|1\rangle + \sin(\frac{\theta}{2})|0\rangle$ where $\theta = \tan^{-1}(2D_{01}\mathcal{E}_z/\omega_{01})$. The expression for ζ in the ground state is therefore

$$\begin{aligned} \zeta(t) = \frac{\left\langle\widetilde{0}\right|D_z\left|\widetilde{0}\right\rangle}{D_{01}} &= -\sin\theta = \frac{-D_{01}\mathcal{E}_z(t)}{\sqrt{[D_{01}\mathcal{E}_z(t)]^2 + (\omega_{01}/2)^2}} \\ &\approx -\frac{2D_{01}\mathcal{E}_0}{\omega_{01}}\cos(\omega t + \beta)\left[1 - \frac{1}{2}\left(\frac{2D_{01}\mathcal{E}_0}{\omega_{01}}\right)^2 \cos^2(\omega t + \beta) + \ldots\right]. \end{aligned} \tag{7}$$

This expression also exhibits the features of $\zeta(t)$ that are relevant to the CT method: (a) the amplitude of ζ approaches 1 when $D_{01}\mathcal{E}_z$ exceeds ω_0, as shown in Fig. 4, and (b) the time-dependence of $\zeta(t)$ contains higher harmonics of ω because of its nonlinear dependence on $\mathcal{E}_z(t)$, as shown in Fig. 5.

C. Suppressing systematics due to the oscillating $\mathcal{E}$-field

We note that an electron EDM precision $\delta d_e = 10^{-31}$ e cm corresponds to a measurement of the P,T-violating Rabi frequency Ω_{PT} with a precision of $\delta\Omega_{PT} = 2\pi \times 0.5$ μHz.

An oscillating $\mathcal{E}$-field in the region occupied by the molecules induces a $\mathcal{B}$-field with amplitude $\mathcal{B}_d \sim \frac{\ell\omega_E}{c^2}\mathcal{E}_0$, where ℓ is a length scale on the order of the electrode size. With $\ell \sim 1$ cm, $\mathcal{E}_0 \sim 2$ kV/cm and $\omega_E = 2\pi\times$ 10 MHz, the

displacement $\mathcal{B}$-field has amplitude $\mathcal{B}_d \sim 10$ mG, which leads to a spurious Rabi frequency $\Omega_d \sim 2\pi\times$ 20 kHz that mimics Ω_{PT}.

This effect can be suppressed in two separate ways. First, we note that the displacement $\mathcal{B}$-field is perpendicular to $\vec{\mathcal{E}}$, which suppresses shifts in ρ_{ee} because $\mathcal{B}$-fields in the xy-plane only couple $|F=0, m_F=0\rangle$ to the $|F'=1, m_{F'}=\pm1\rangle$ levels. Further, the $|F=0, m_F=0\rangle \rightarrow |F'=1, m_{F'}=\pm1\rangle$ transitions are out of resonance with the frequency $\omega_E = \omega_0$ due to the tensor Stark shift in polar molecules [39–41].

Any residual $\mathcal{B}$-field component along $\hat{z}$, for example due to electrode mis-alignment, can be suppressed using a second mechanism. Note that the induced $\mathcal{B}$-field is proportional to the time derivative of $\mathcal{E}_z$, and so it lags the applied $\mathcal{E}$-field in phase by $\pi/2$. For example, if $\vec{\mathcal{B}}_d \cdot \hat{z} \neq 0$ and β is set to $\pm\frac{\pi}{2}$, the change in ρ_{ee} depends on whether the $\mathcal{E}$-field is on or off. Such a shift is *only* produced when $\vec{\mathcal{B}}_d \cdot \hat{z} \neq 0$, and is therefore a clean diagnostic for displacement $\mathcal{B}$-fields.

Despite these two suppression mechanisms, it is possible that a combination of phase errors (e.g., due to charging currents or cable impedance mismatches) and electrode misalignments could lead to a residual $\mathcal{B}$-field that is both parallel to $\hat{z}$ and in phase with $\mathcal{E}_z$. For example misalignment of the rf electric and magnetic field directions by $\theta = 10^{-5}$ rad, and a phase error in the electric field drive of $\Delta\beta = 10^{-5}$ rad will lead to a residual Rabi frequency $\Omega'_d \sim \theta\ \Delta\beta\ \Omega_d = 2\pi \times 10^{-6}$ Hz. This small error can be detected and further suppressed using the sub-harmonic modulation method described next.

As noted in the main text, the molecular orientation ζ is *nonlinear* in $\mathcal{E}_z$. If $\mathcal{E}_0$ is large enough to appreciably polarize the molecule, then $\zeta(t)$ also contains higher odd harmonics of ω_E (see Fig. 5). This fact leads to a unique and powerful diagnostic for systematic errors: an EDM search experiment can be conducted using, e.g., $\omega_E = \omega_0/3$ and $\omega_B = \omega_0$. Any induced magnetic fields that are linear in $\mathcal{E}_z$ (a condition which covers the majority of conceivable systematics) oscillate at $\omega_0/3$, far off resonance from the clock transition, and so their interference with the transition amplitude is significantly suppressed. On the other hand, the fourier component of ζ that oscillates at $3\omega_E = \omega_0$ (with amplitude ζ_3) resonantly contributes to the transition probability as $\rho_{ee}(\tau) = \sin^2\left[\frac{(\Omega_B + \Omega_{PT,3}\ \cos 3\beta)\,\tau}{2}\right]$, with $\Omega_{PT,3} = \frac{1}{2}W_{PT}\zeta_3$. Therefore, driving the electric field at a sub-harmonic of ω_0 offers a convenient diagnostic to discriminate between systematic errors and real P,T-violating signals. Since $\zeta_3 < \zeta_0$ though, it yields lower EDM sensitivity, so we envision that experiments using the proposed method will intersperse some measurements with $\omega_E = \omega_0/3$ as systematic checks within larger measurement blocks with $\omega_E = \omega_0$.

D. Differential Stark shift

Under the influence of the electric field $\mathcal{E}_z(t) = \mathcal{E}_0 \cos(\omega t + \beta)$, there is a small differential Stark shift (DSS) between the hyperfine clock states $|g\rangle, |e\rangle$. This shift arises due to a combination of the $E1$ interaction of the molecular dipole moment with the electric field, the spin-rotation interaction, and the hyperfine interaction. From perturbation theory, we find that the resulting change in the hyperfine resonance frequency ω_0 is

$$\Delta\omega_{\mathrm{DSS}} \sim \frac{\gamma^2\, b}{B_{\mathrm{rot}}^4}\,(D\mathcal{E}_0)^2 \cos^2(\omega t + \beta). \tag{8}$$

We have also confirmed this expression with direct numerical calculations using the Hamiltonian in Equation 5.

The static part of $\Delta\omega_{\mathrm{DSS}}$ can be absorbed into the definition of the resonance frequency ω_0, leaving a modulation of the hyperfine splitting at a frequency 2ω. Therefore the effect of the DSS can be described by writing the resonance frequency as $\omega'_0 = \omega_0\,[1 + h\cos(2\omega t + 2\beta)]$, where h is a dimensionless parameter. The numerically calculated value of h is $\sim 10^{-6}$ at $\mathcal{E}_0 \sim 2$ kV/cm for YbAg. It now remains to consider the effect of such a modulation of the resonance frequency on the time-evolution of $\rho_{ee}(t)$.

The Rabi problem for a two-level system with a modulated resonance frequency has not appeared in the literature to the best of our knowledge (although the Rabi problem with a frequency-modulated drive frequency is well-understood, cf. [42]). Therefore we briefly describe the method of solution here.

We work in the interaction picture, wherein the magnetic dipole moment operator is represented by the matrix

$$\mu_z = \begin{pmatrix} 0 & \mu_{ge}\, e^{-i\int \omega'_0\, dt} \\ \mu_{eg}\, e^{+i\int \omega'_0\, dt} & 0 \end{pmatrix} = \begin{pmatrix} 0 & \mu_{ge}\, e^{-i\omega_0 t}\, e^{+i\frac{h\omega_0}{2\omega}\sin(2\omega t + 2\beta)} \\ \mu_{eg}\, e^{+i\omega_0 t}\, e^{-i\frac{h\omega_0}{2\omega}\sin(2\omega t + 2\beta)} & 0 \end{pmatrix} \tag{9}$$

in the two-level subspace spanned by $|g\rangle, |e\rangle$. The Hamiltonian for the hyperfine transition is

$$H'_{\mathrm{hf}} = -\mu_z \mathcal{B}_0 \cos\omega t = \Omega_B \begin{pmatrix} 0 & e^{-i\omega_0 t}\, e^{+i\frac{h\omega_0}{2\omega}\sin(2\omega t + 2\beta)} \\ e^{+i\omega_0 t}\, e^{-i\frac{h\omega_0}{2\omega}\sin(2\omega t + 2\beta)} & 0 \end{pmatrix} \cos\omega t. \tag{10}$$

Following the usual approach to the rotating-wave approximation, we retain just the slowest terms in this Hamiltonian. We also expand the phase modulation term up to $\mathcal{O}(h^2)$ owing to the smallness of h, and get

$$H'_{\rm hf} \approx \frac{\Omega_B}{2}\begin{pmatrix} 0 & e^{+i\Delta t}\left[1+\left(\frac{h\omega_0}{4\omega}\right)e^{i2\beta}\right] \\ e^{-i\Delta t}\left[1+\left(\frac{h\omega_0}{4\omega}\right)e^{-i2\beta}\right] & 0 \end{pmatrix} = \frac{1}{2}\begin{pmatrix} 0 & \Omega_M\, e^{+i\Delta t} \\ \Omega_M^*\, e^{-i\Delta t} & 0 \end{pmatrix}. \tag{11}$$

This has exactly the same form as the Hamiltonian for the standard Rabi problem with a fixed hyperfine splitting, $H_{\rm hf} = \frac{1}{2}\begin{pmatrix} 0 & \Omega_B\, e^{+i\Delta t} \\ \Omega_B^*\, e^{-i\Delta t} & 0 \end{pmatrix}$. Importantly, this means $\rho_{ee}(t)$ evolves in time in just the same way as in the unmodulated case. The only difference is that the Rabi frequency is modified to $\Omega_M = \Omega_B\left[1+\left(\frac{h\omega_0}{4\omega}\right)e^{i2\beta}\right]$. Direct numerical solutions of the Schrodinger equation with a modulated resonance frequency confirm this simple picture.

The shift in the measured Rabi frequency on resonance is then $\Omega_{\rm DSS} = \frac{h}{4}\Omega_B\cos 2\beta$. With $\Omega_B = \pi/2\tau = 2\pi\times 25$ mHz and $h = 10^{-6}$, this evaluates to $\Omega_{\rm DSS} \sim 2\pi\times 6$ nHz $\cos 2\beta$, which is an extremely small effect compared to the targeted precision $\delta\Omega_{PT} \sim 2\pi\times$ 500 nHz.

Nevertheless, we show how it can be suppressed further. Note that due to its $\cos 2\beta$ dependence, this shift is the same for $\beta = 0$ and $\beta = \pi$, whereas the PT-violating observable $\Omega_{PT}\cos\beta$ switches sign between these two phases. Further note that $\Omega_{\rm DSS} \propto \Omega_B \propto \mathcal{B}_0$. Therefore measurements of $\rho_{ee}(\tau)$ with different values of $\Omega_B\tau$ (say $\frac{\pi}{2}$ and $\frac{5\pi}{2}$) can distinguish a genuine PT-violating signal from DSS-induced transition amplitudes. These, in combination with the other diagnostics described above (e.g., sub-harmonic drive, electric field amplitude variation) at our disposal, lead us to conclude that DSS effects can be cleanly distinguished from a true P,T-violating signal.

E. A menu of molecules for P,T-violation searches

As an illustration of the variety of polar molecules to which the clok transition method can be applied, the following tables list neutral molecules (Table I) and singly-charged molecular ions (Table II) that can be used to search for electron and nuclear P,T-violation with the CT method. In each table, a combination of the atoms from the two columns forms an EDM-sensitive molecule to which the CT method can be applied. Atoms that can be cooled to ultracold temperatures are shown in bold: ultracold assembled molecules can be produced from pairs of these.

The tables include molecules that have been previously used (YbF [3]) or proposed for use in EDM experiments (HgF, HgCl, HgBr [43], HgNa, HgK, HgRb [23], RaF [44], BaF [45], RaAg [25], HgCa [46]). The tables are by no means exhaustive – other molecules can be used as well (e.g., TlF, ^{225}Ra^{199}Hg).

TABLE I: Neutral molecules.

Electron EDM

$^{138}\mathbf{Ba}$	^{19}F
$^{174}\mathbf{Yb}$	^{35}Cl
$^{202}\mathbf{Hg}$	^{79}Br
$^{226}\mathbf{Ra}$	$^{107,109}\mathbf{Ag}$
	^{16}O^{1}H

Nuclear EDM

$^{199}\mathbf{Hg}$	^{17}O
^{207}Pb	^{33}S
$^{225}\mathbf{Ra}$	$^{43}\mathbf{Ca}$
	$^{87}\mathbf{Sr}$

TABLE II: Molecular ions.

Electron EDM

^{200}Hg	^{17}O
^{226}Ra	^{33}S
^{208}Pb	^{43}Ca
^{232}Th	^{87}Sr

Nuclear EDM

^{133}Ba	^{19}F
^{199}Hg	^{35}Cl
^{207}Pb	^{79}Br
^{225}Ra	^{16}O^{1}H
^{229}Pa	
^{229}Th	